Supplemental File 2 (S02) for

Integration of microscopy and multi-omic data reveals pathology of a coral disease outbreak

Carly E. Karrick[1,2]*, Hannah L. Swain[3]*, Ashley M. Rossin[4,5], Mallory Kastner[6,7], Gillian Coleman[5,8], Morgan Coleman[5, 9], Lauren I. Howe-Kerr[2,10], Michelle A. Johnston[11], Matthew D. Meyer[12], Marissa F. Nuttall[11], Mia K. Olson[2], Amy Apprill[6], Marilyn Brandt[8], Daniel M. Holstein[5,13], Laura Mydlarz[3], Adrienne M.S. Correa[1,2]

[1]Department of Environmental Science, Policy, and Management, University of California, Berkeley, CA, USA
[2]Biosciences Department, Rice University, Houston, TX, USA
[3]Department of Biology, The University of Texas at Arlington, TX, USA
[4]Cooperative Institute for Marine & Atmospheric Studies, University of Miami, FL, USA
[5]Department of Oceanography & Coastal Sciences, Louisiana State University, Baton Rouge, LA, USA
[6]Department of Marine Chemistry and Geochemistry, Woods Hole Oceanographic Institution, Woods Hole, MA, USA
[7]MIT-WHOI Joint Program in Oceanography/Applied Ocean Science and Engineering, Earth, Atmospheric and Planetary Sciences, Cambridge and Woods Hole, MA, USA
[8]Center for Marine and Environmental Studies, University of the Virgin Islands, USVI, USA
[9]Harte Research Institute, Texas A&M University-Corpus Christi, Corpus Christi, TX, USA
[10]Minderoo Foundation, Perth, WA, Australia
[11]National Oceanic and Atmospheric Administration (NOAA) Office of National Marine Sanctuaries, Flower Garden Banks National Marine Sanctuary, Galveston, TX, United States,
[12]Shared Equipment Authority, Rice University, Houston, TX, USA
[13]School of Marine and Atmospheric Sciences, Stony Brook University, Stony Brook, NY, USA

*Co-first authors

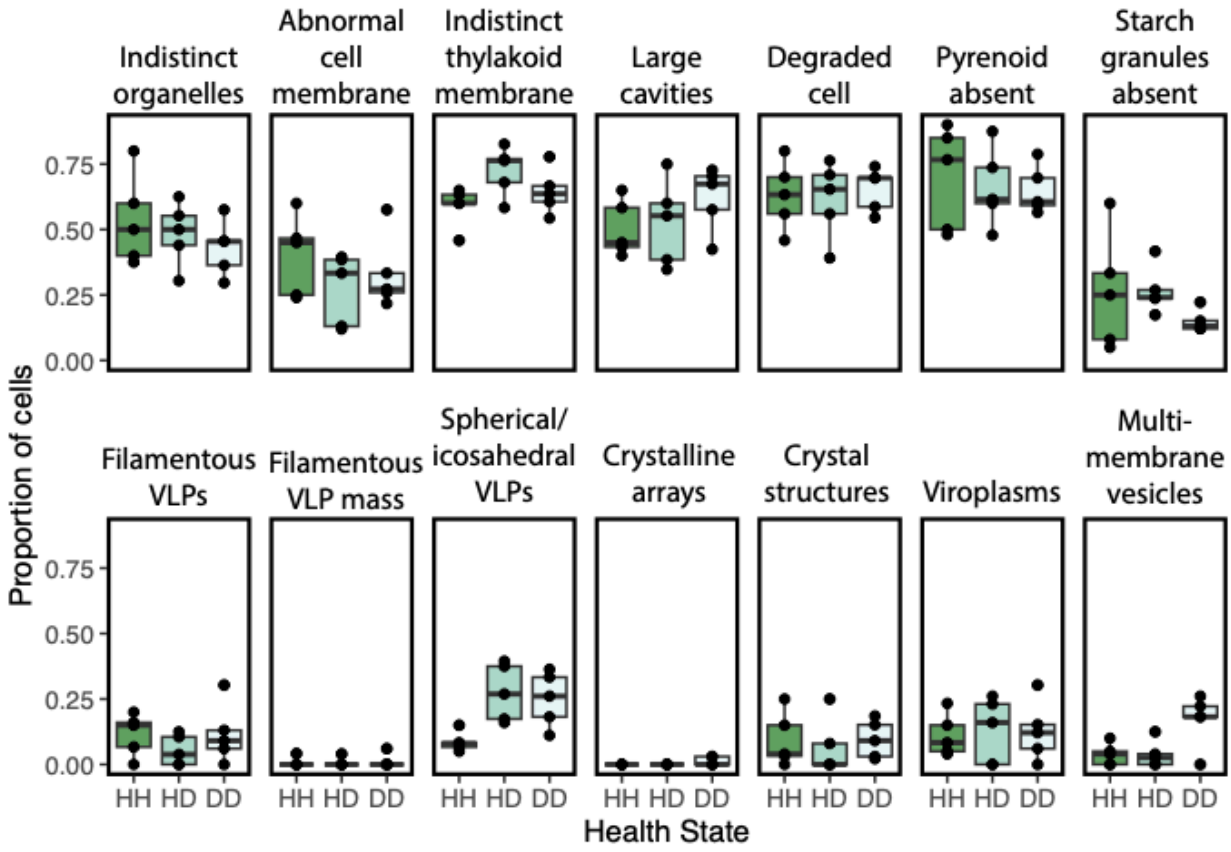

Supplemental Figure 1: Boxplots of the proportion of cells per tissue health state with each feature analyzed in Symbiodiniaceae electron micrographs taken with transmission electron microscopy (TEM). HH: apparently healthy tissue on an apparently healthy coral; HD: apparently healthy tissue on a diseased coral; DD: lesion-adjacent tissue; VLP: virus-like particle.

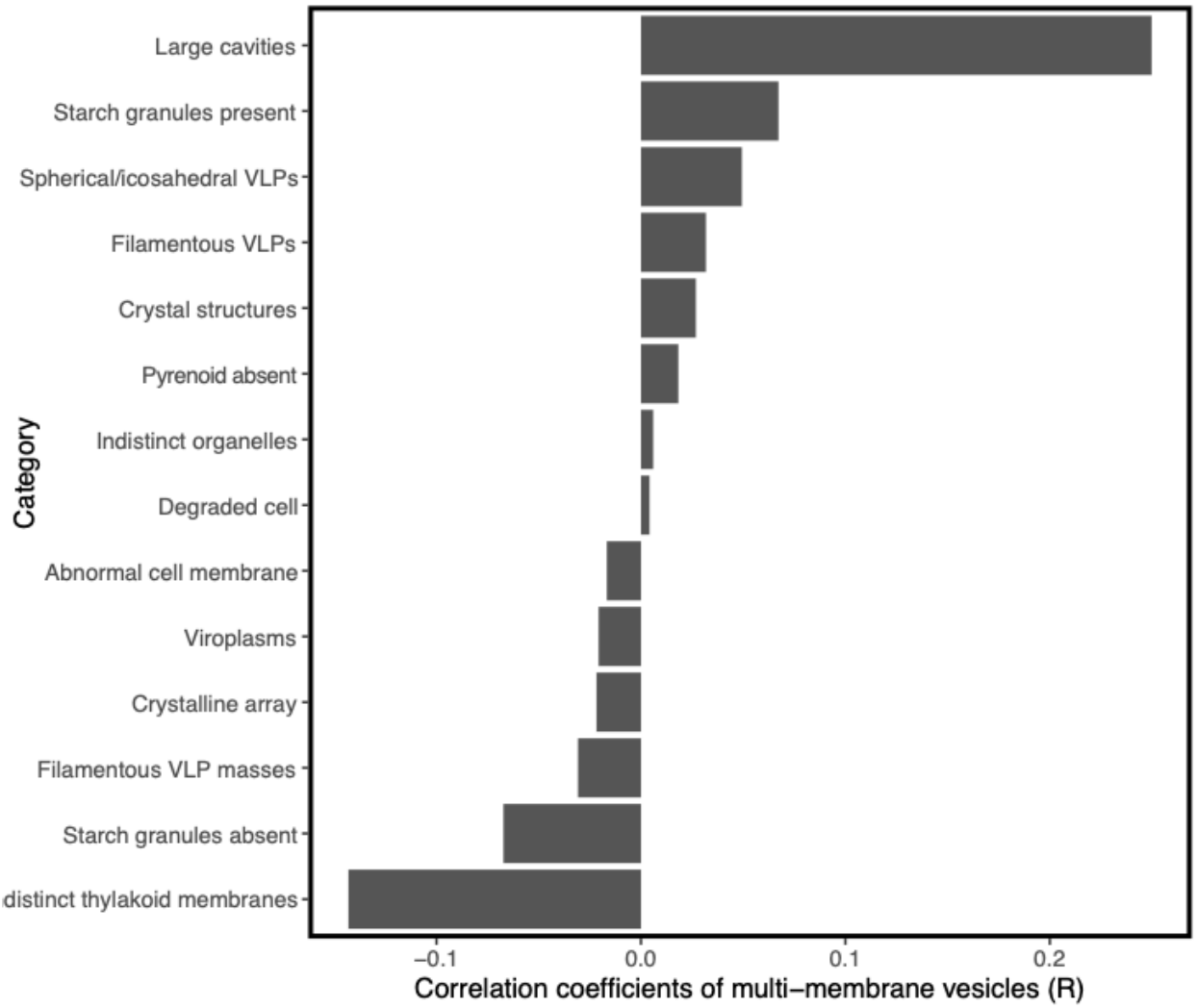

Supplemental Figure 2: The Pearson's correlation coefficients (R) between multi-membrane vesicles and other features analyzed in electron micrographs of Symbiodiniaceae cells captured with transmission electron microscopy (TEM). VLP: virus-like particle.

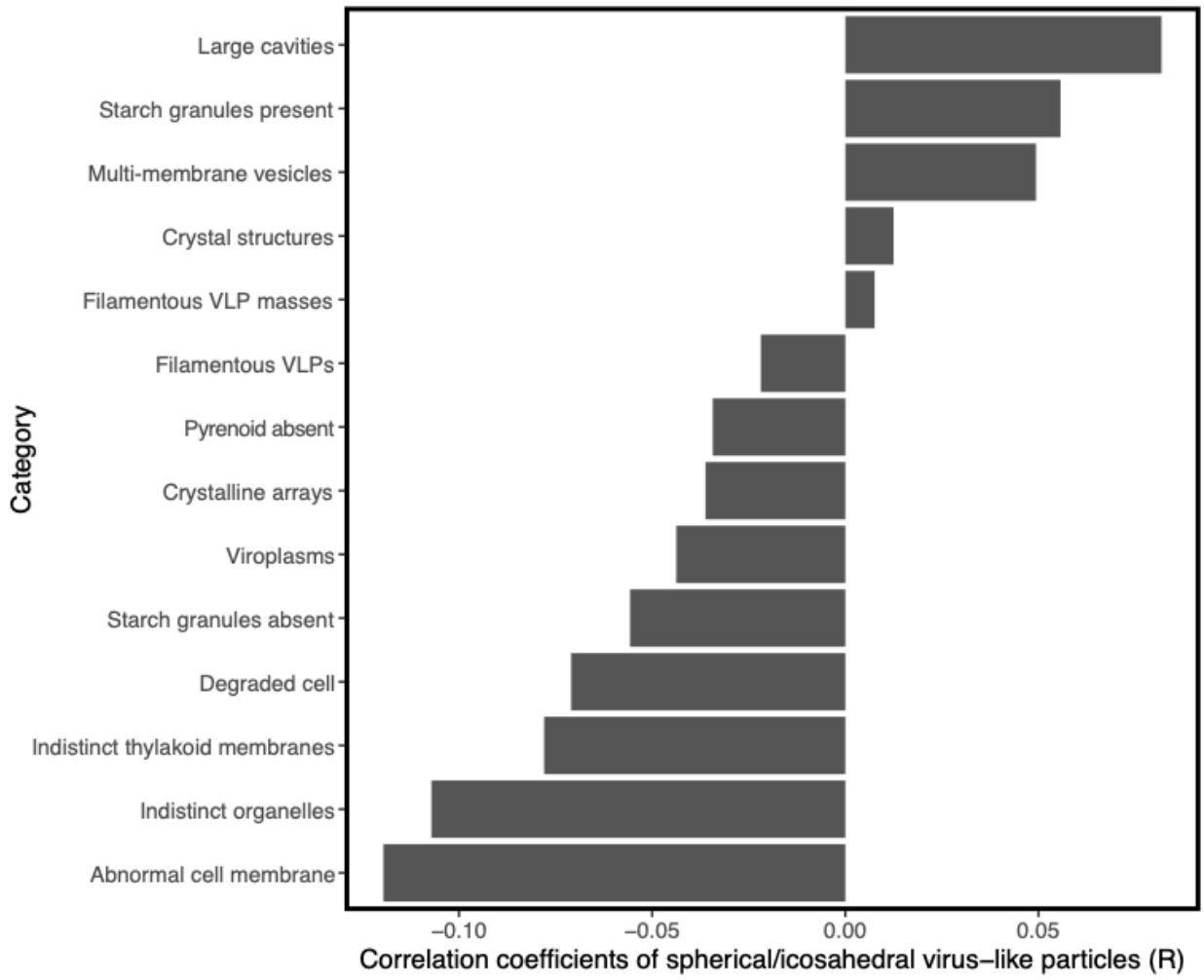

Supplemental Figure 3: The Pearson's correlation coefficients (R) between spherical/icosahedral virus-like particles (VLPs) and other features analyzed in electron micrographs of Symbiodiniaceae cells captured with transmission electron microscopy (TEM).

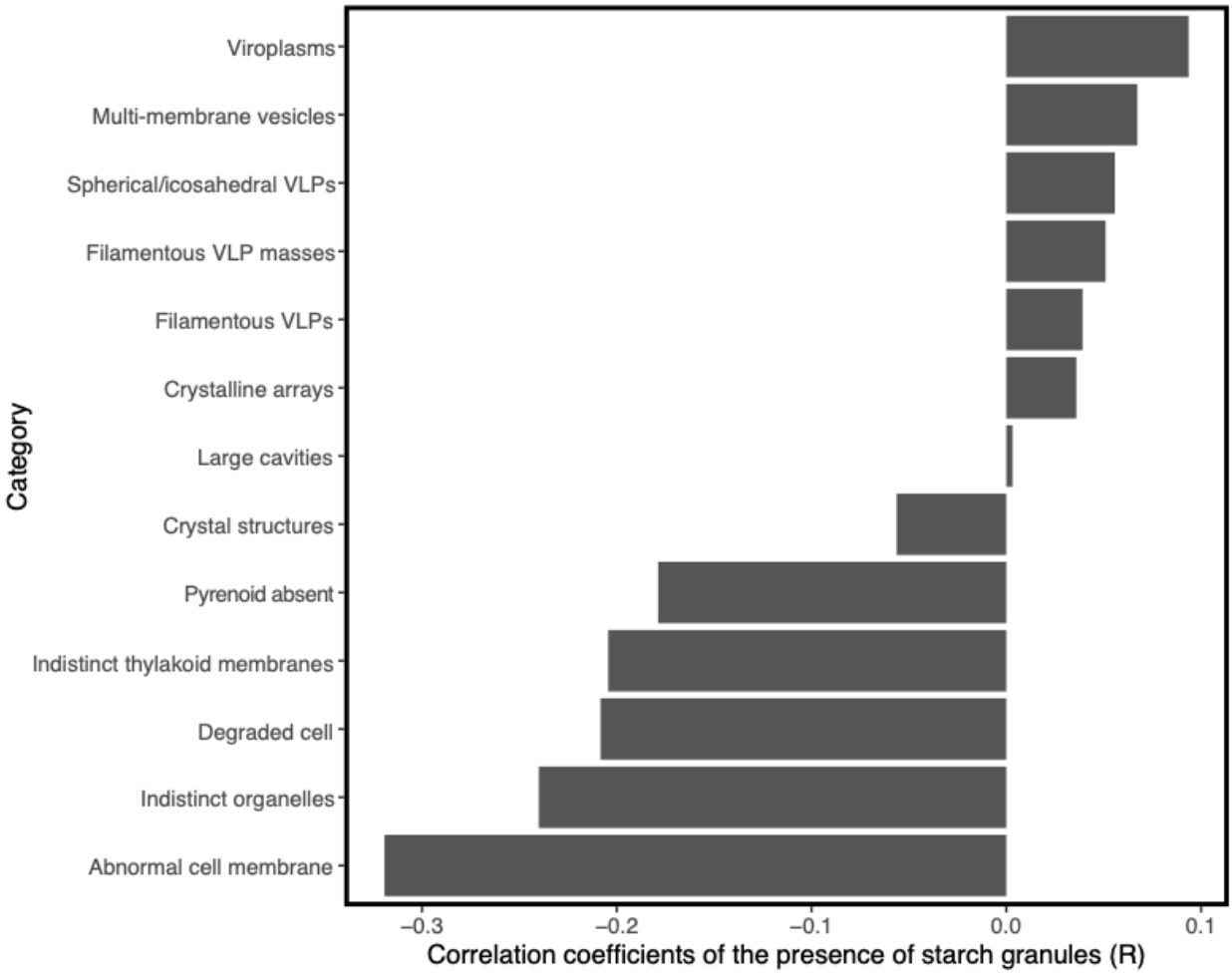

Supplemental Figure 4: The Pearson's correlation coefficients (R) between the presence of starch granules and other features analyzed in electron micrographs of Symbiodiniaceae cells captured with transmission electron microscopy (TEM). VLP: virus-like particle.

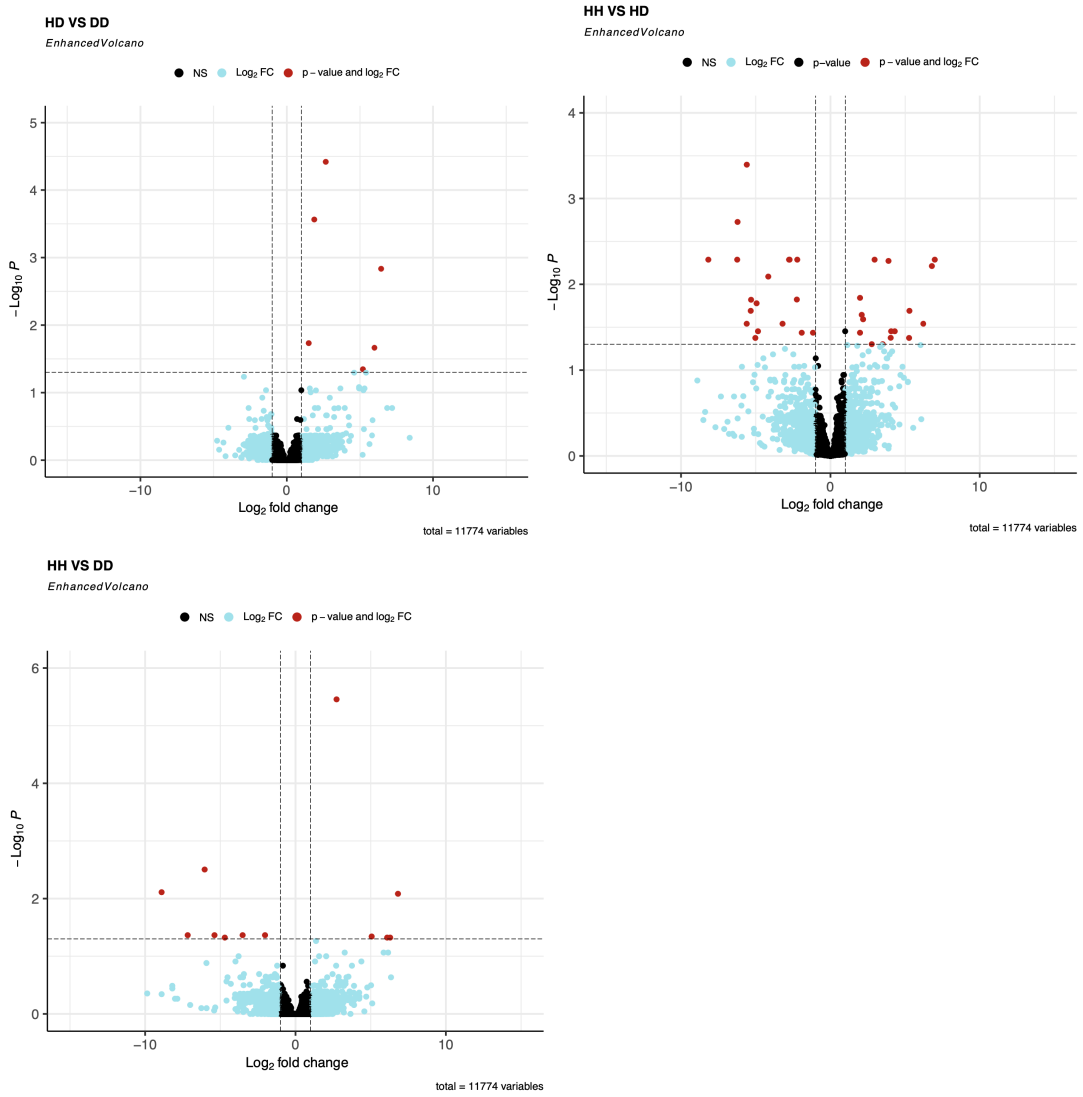

Supplemental Figure 5: *Pseudodiploria strigosa* differential expression and log2fold change volcano plots across DESeq2 contrast arguments: HH vs DD, HH vs HD, HD vs DD.

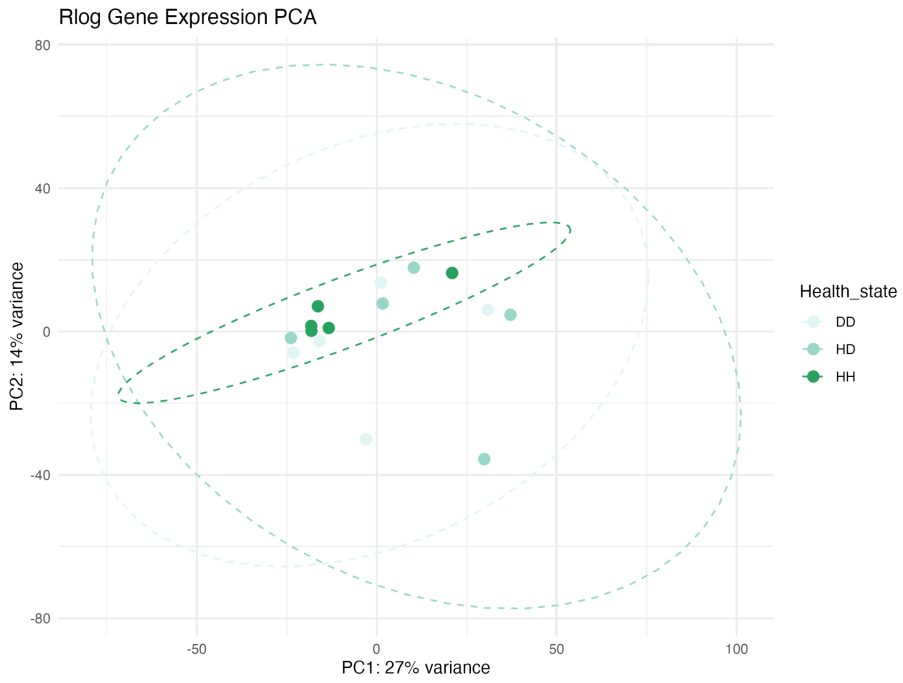

Supplemental Figure 6: Principal component analysis of *Pseudodiploria strigosa* samples across health states: HH: apparently healthy tissue on an apparently healthy coral; HD: apparently healthy tissue on a diseased coral; DD: lesion-adjacent tissue.

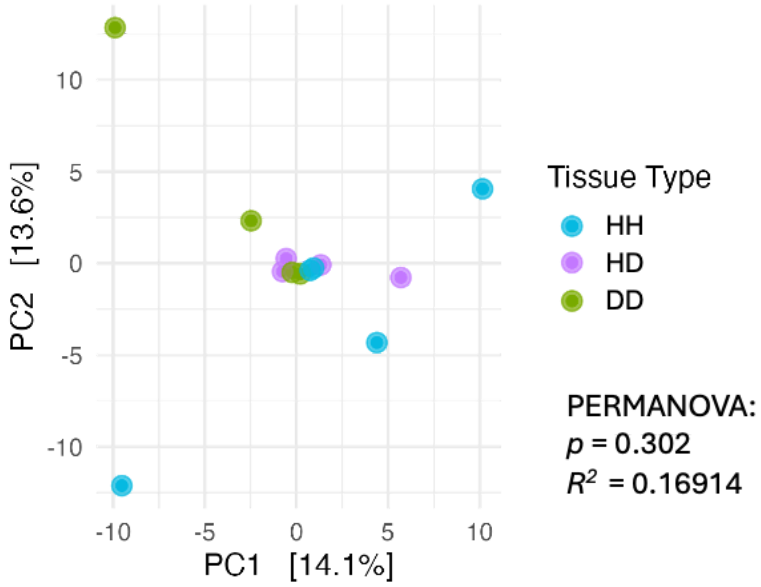

Supplementary Figure 7: There is no uniformity within the *Pseudodiploria strigosa* tissue bacterial/archaeal community across all tissue health types based on sequencing of the 16S rRNA gene. Principal Component Analysis of *P. strigosa* tissue bacterial/archaeal communities, colored by tissue types (HH: blue, HD: purple, DD: green). PERMANOVA by tissue type: p =

0.302, R^2 = 0.16914. HH: apparently healthy tissue on an apparently healthy coral; HD: apparently healthy tissue on a diseased coral; DD: lesion-adjacent tissue.

Supplemental Figure 8: Mapped genomes of two viral operational taxonomic units (vOTUs) rated as having high quality genomes based on CheckV: (A) vOTU_20 and (B) vOTU_27. ORF: open reading frame.

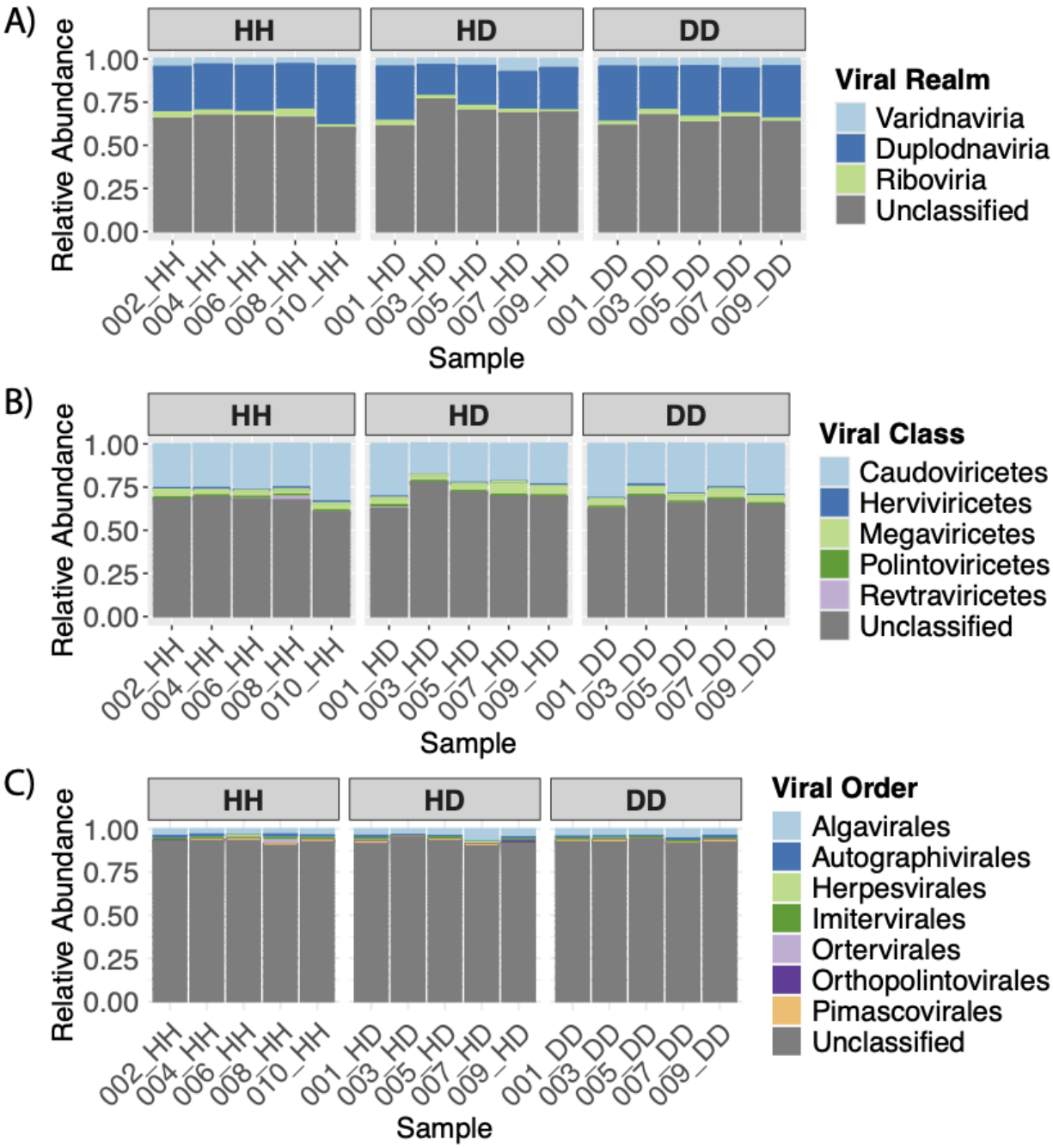

Supplemental Figure 9: The relative abundance of viral operational taxonomic units (vOTUs) per sample, plotted at the (A) Realm, (B) Class, and (C) Order levels.

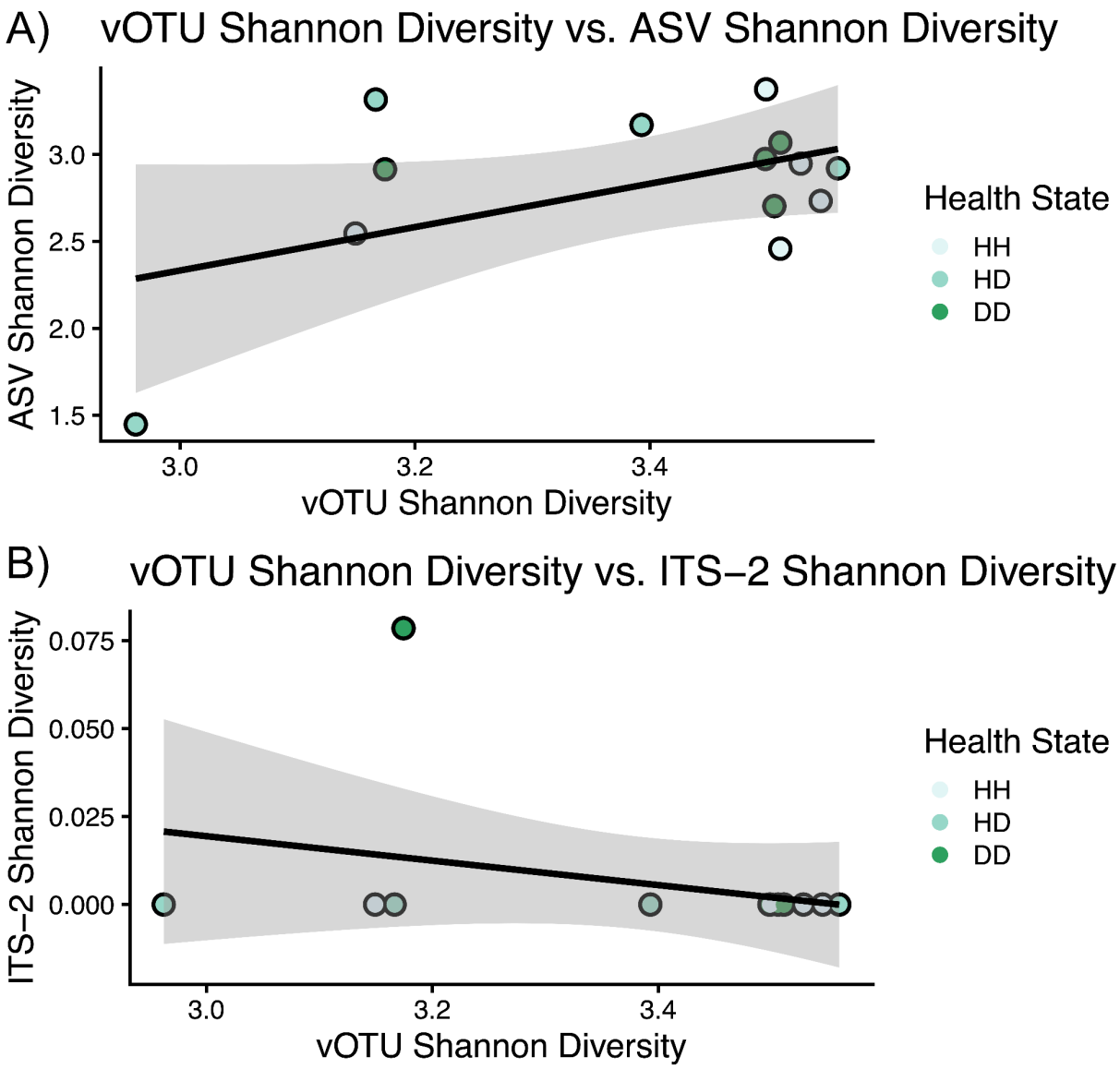

Supplemental Figure 10: Shannon diversity indices of viral operational taxonomic units (vOTUs) mined from bulk RNA-Seq data versus those of (A) amplicon sequence variants (ASVs) identified from sequencing of the v4 region of the 16S rRNA gene and (B) ITS-2 type profiles identified from sequencing of the internal transcribed spacer-2 (ITS-2) region of Symbiodiniaceae rDNA. Points are fit with a LOESS trendline and colored by health state. HH: apparently healthy tissue on an apparently healthy coral; HD: apparently healthy tissue on a diseased coral; DD: lesion-adjacent tissue on a diseased coral.

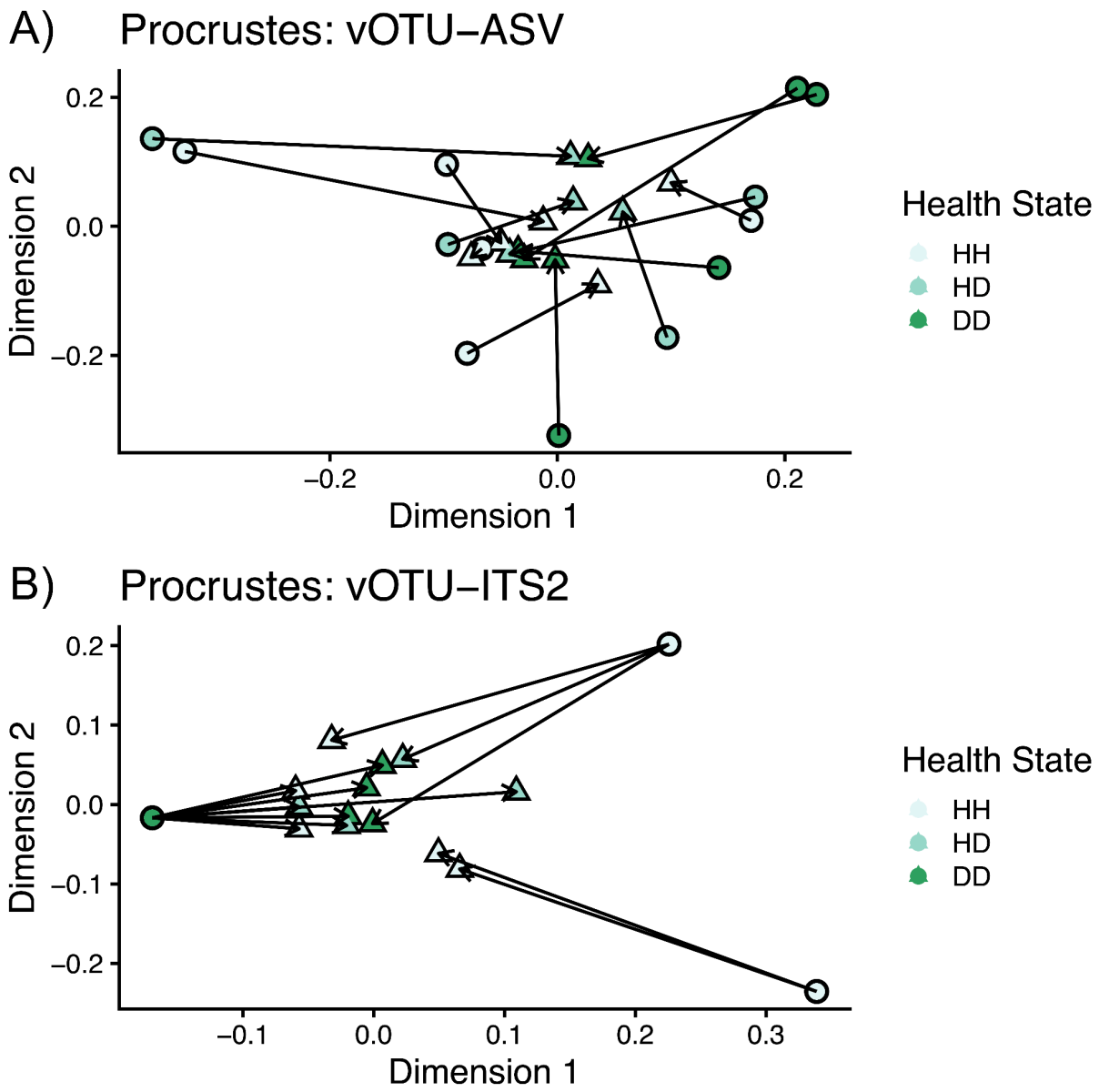

Supplemental Figure 11: Results of Procrustes analyses of principal coordinate analysis (PCoA) ordinations of Bray-Curtis dissimilarity matrices generated from counts of viral operational taxonomic units (vOTUs) mined from bulk RNA-Seq data versus those of (A) amplicon sequence variants (ASVs) identified from sequencing of the v4 region of the 16S rRNA gene and (B) ITS-2 type profiles identified from sequencing of the internal transcribed spacer-2 (ITS-2) region of Symbiodiniaceae rDNA. Arrows connect a sample's corresponding vOTU ordination (triangle) and (A) ASV or (B) ITS-2 ordination (circles), where longer arrows indicate less overlap in ordinations. All points are colored by health, where HH: apparently healthy tissue on an apparently healthy coral; HD: apparently healthy tissue on a diseased coral; DD: lesion-adjacent tissue on a diseased coral.

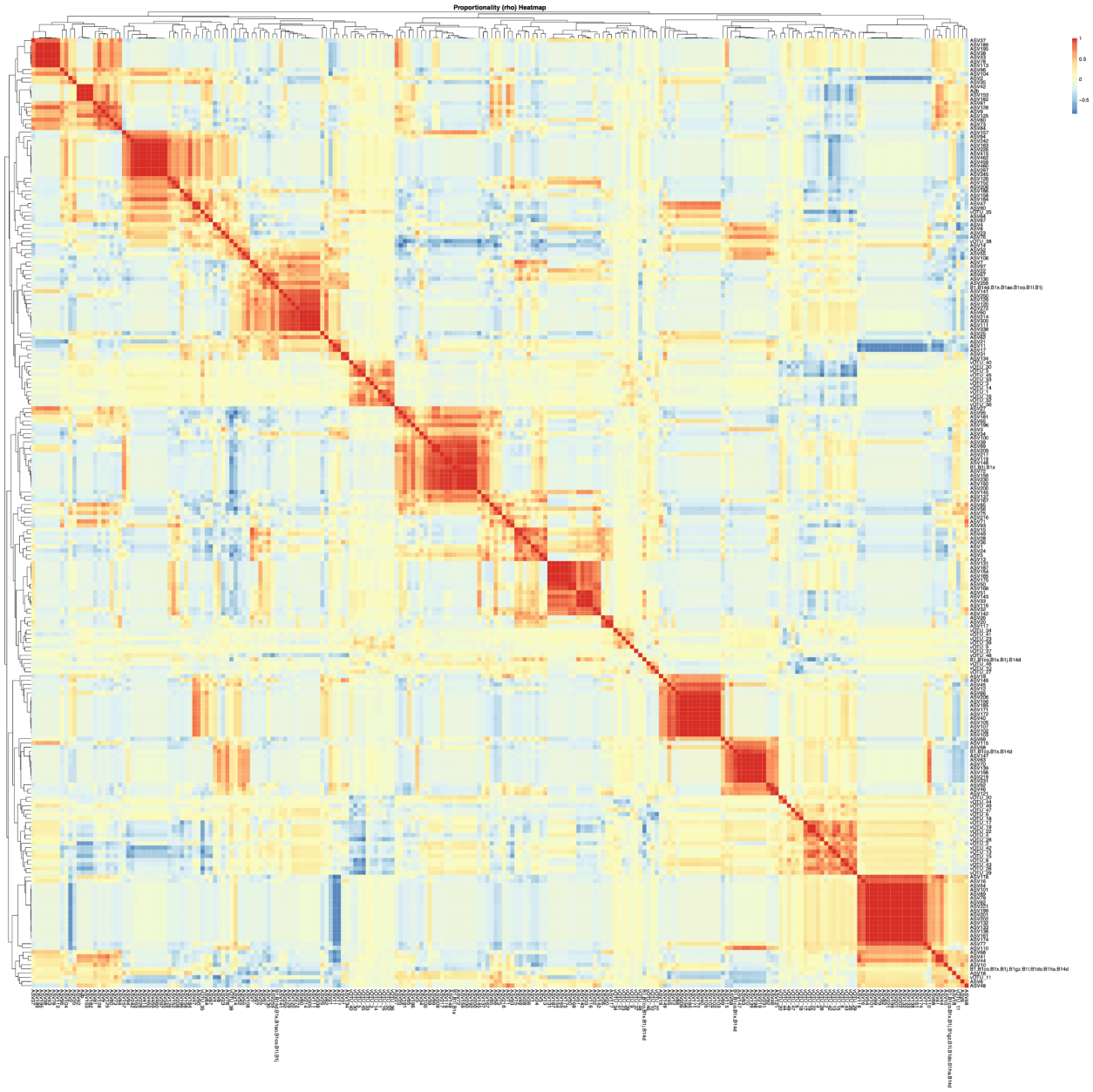

Supplemental Figure 12: Heatmap showing proportionality between microbial taxa in global pairwise comparisons of all amplicon sequence variants (ASVs) generated from sequencing of the v4 region of the 16S rRNA gene, ITS-2 type profiles generated from sequencing of the internal transcribed spacer-2 (ITS-2) region of Symbiodiniaceae rDNA, and viral operational taxonomic units (vOTUs) mined from bulk RNA-Seq data. All microbe-microbe relationships with rho > 0.7 are shown.

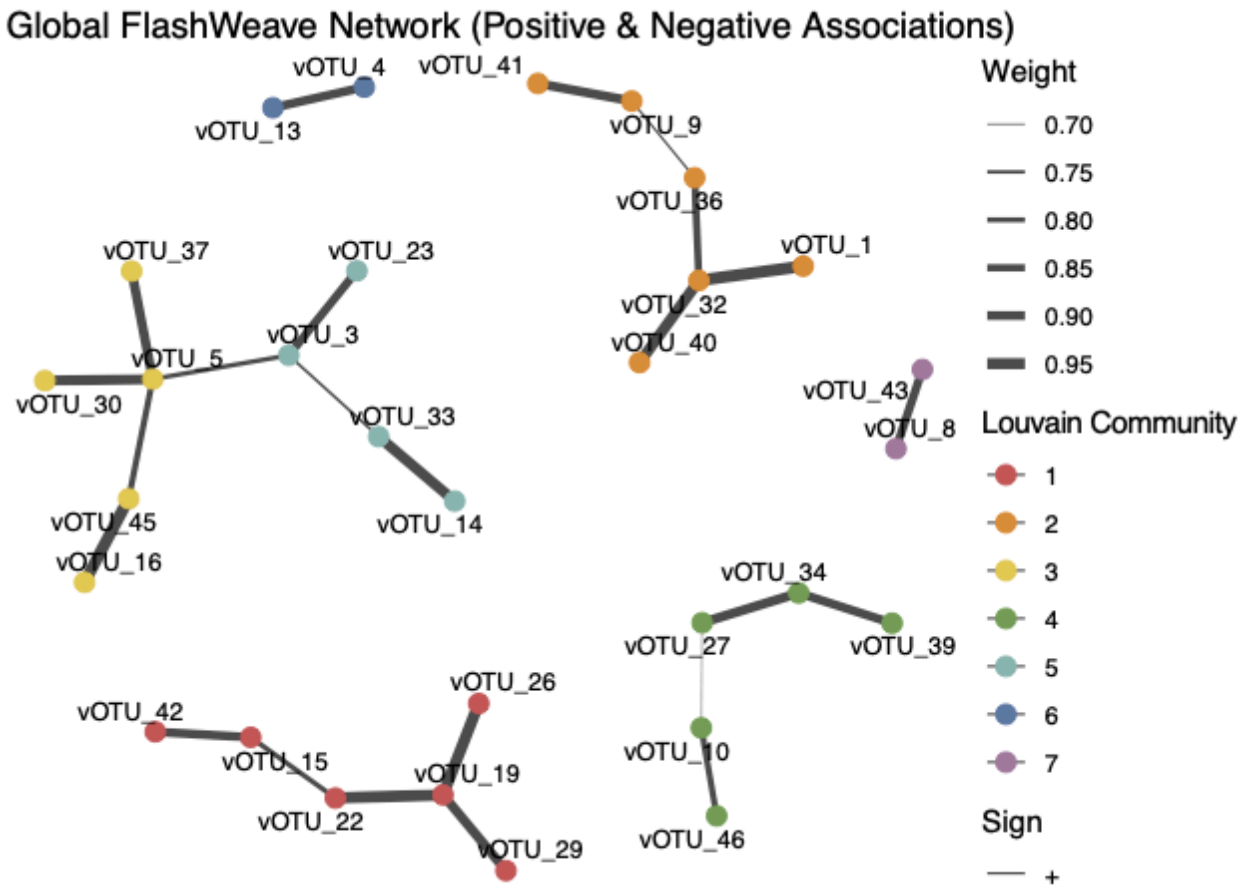

Supplemental Figure 13: Global co-occurrence network created from all samples. The network combines associations between amplicon sequence variants (ASVs) from sequencing of the v4 region of the 16S rRNA gene, ITS-2 type profiles from sequencing of the internal transcribed spacer 2 (ITS-2) region of Symbiodiniaceae rDNA, and mining of viral OTUs (vOTUs) from bulk RNA-Seq data. Nodes are represented by circles colored by the associated Louvain community. Edges are colored by sign, and edge thickness indicates the absolute value of the weight of the association.

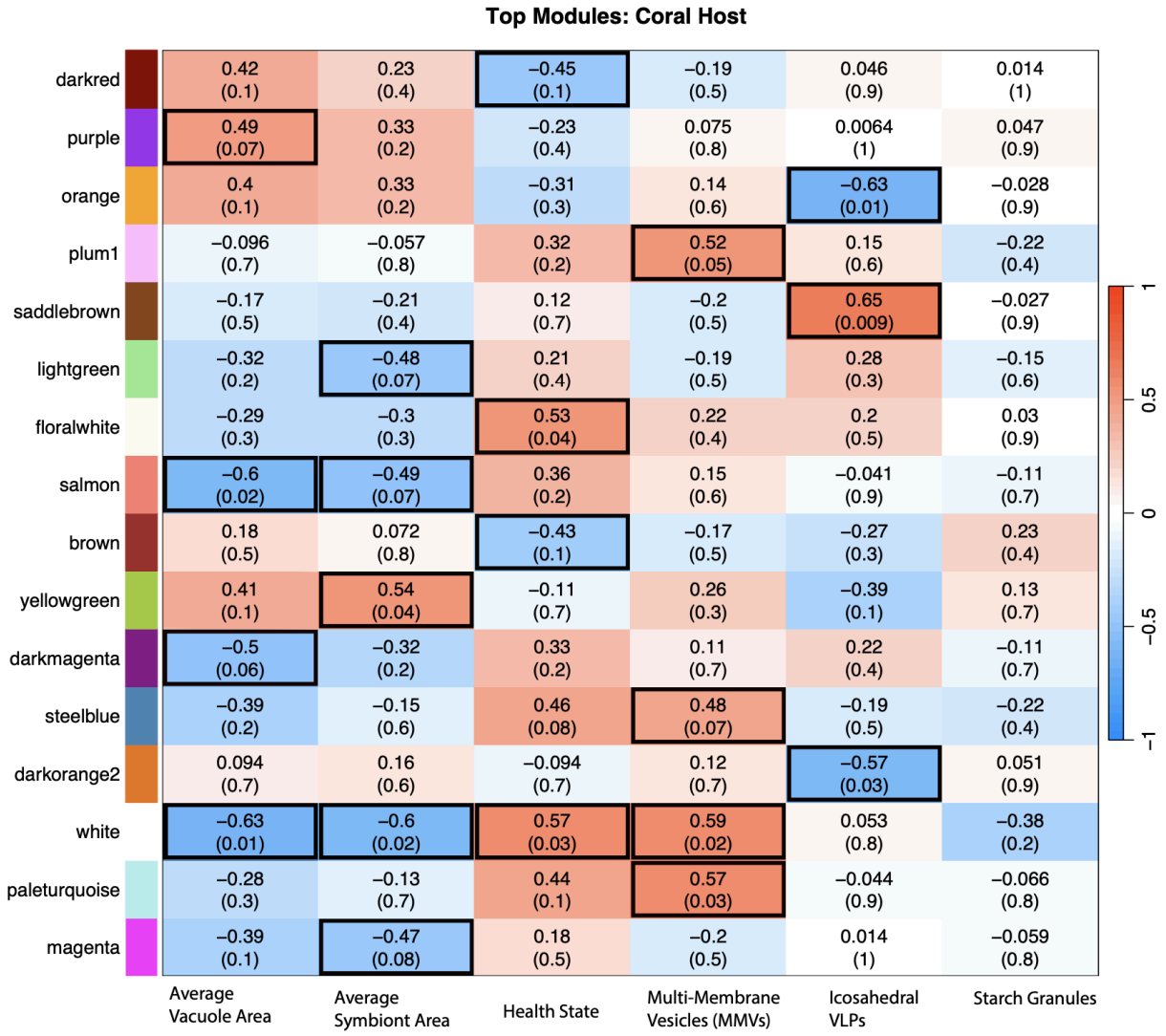

Supplemental Figure 14: Top 17 modules from a Weight Gene Co-Expression Analysis (WGCNA) of *Pseudodiploria strigosa* and correlations to microscopy phenotypes from histology and transmission electron microscopy. Top modules are highlighted and were used for gene ontology enrichments.

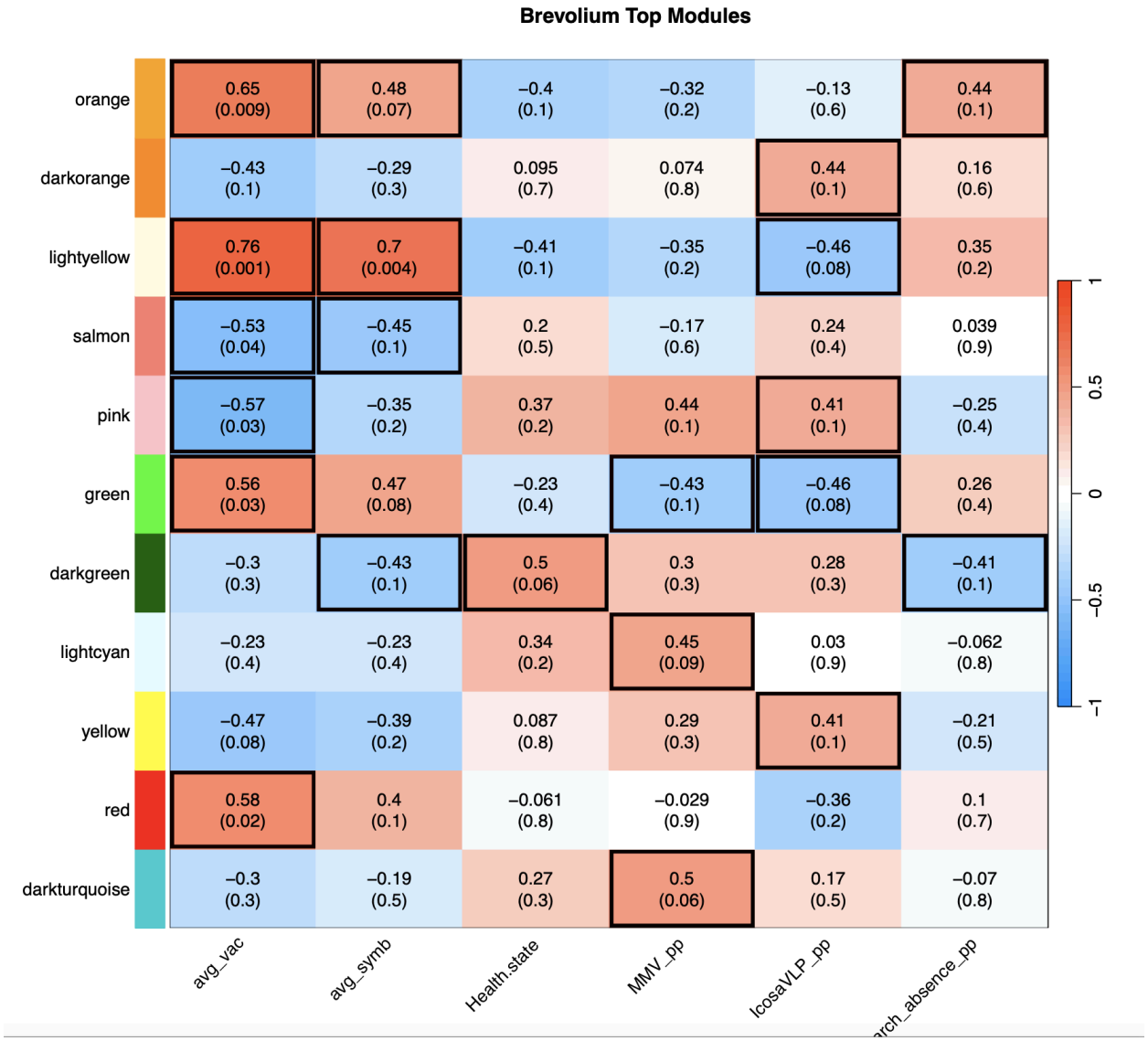

Supplemental Figure 15: Top 11 modules from a Weight Gene Co-Expression Analysis (WGCNA) of *Breviolum* and correlations to microscopy phenotypes from histology and transmission electron microscopy. Top modules are highlighted and were used for gene ontology enrichments.

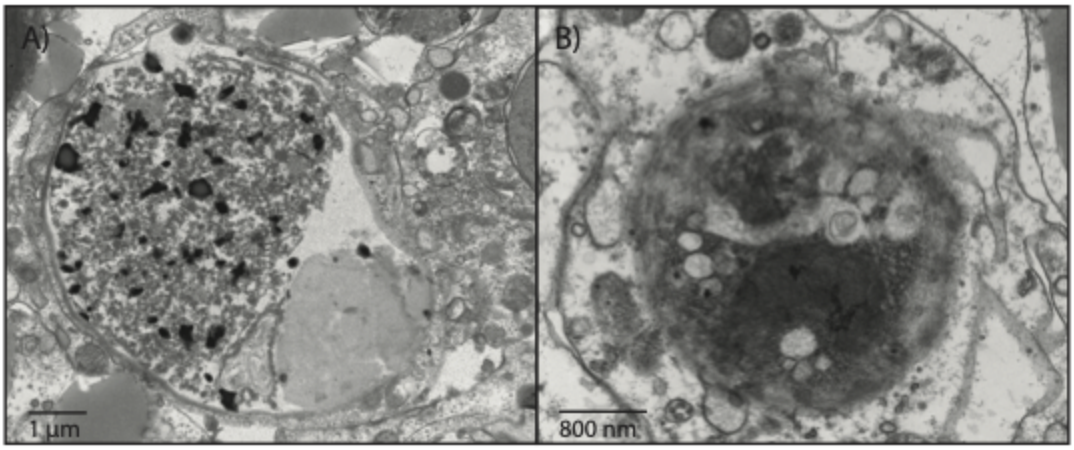

Supplemental Figure 16: Representative electron micrographs from transmission electron microscopy (TEM) of Symbiodiniaceae cells showing examples of cells considered too degraded to score and include in downstream analyses. These cells are mostly full of debris, precluding discerning cellular features. The scale bar in (A) is 1 µm and the scale bar in (B) is 800 nm.

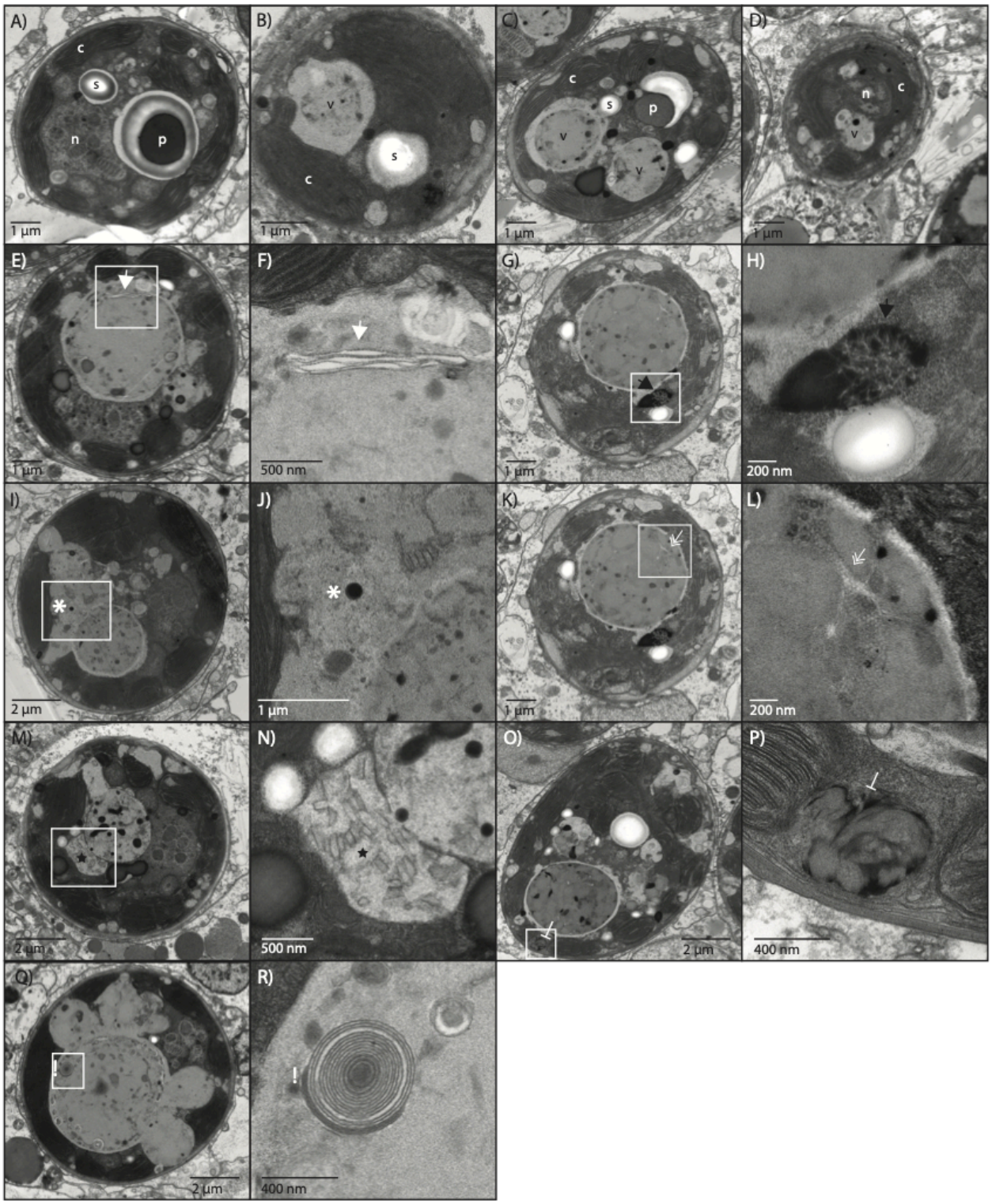

Supplemental Figure 17: Representative electron micrographs of Symbiodiniaceae cells imaged with transmission electron microscopy (TEM). Symbiodiniaceae cells were scored for the presence of various abnormalities potentially indicative of degradation and/or viral infection. (A) A healthy Symbiodiniaceae cell. (B) A degraded Symbiodiniaceae cell, with indistinct

organelles, indistinct thylakoid membranes, and a large cavity/vacuole. (C) A degraded Symbiodiniaceae cell with an abnormal (elongated) cell membrane and two large cavities. (D) A degraded cell with no pyrenoid body or starch granules. (E) A cell containing a filamentous virus-like particle (VLP). (F) An inset of E. (G) A cell containing a mass of filamentous VLPs. (H) An inset of G. (I) A cell containing a spherical/icosahedral VLP. (J) An inset of I. (K) A cell containing a crystalline array of spherical/icosahedral VLPs. (L) An inset of K. (M) A cell containing a crystal structure. (N) An inset of M. (O) A cell containing a whirled viroplasm. (P) An inset of O. (Q) A cell containing a multi-membrane vesicle (MMV). (R) An inset of Q. Abbreviations and symbols are as follows: c: chloroplast; n: nucleus; p: pyrenoid body; s: starch granule; v: vacuole; white arrow: filamentous VLP; black arrow: mass of filamentous VLPs; white asterisk: spherical/icosahedral VLP; white double arrow: crystalline array of spherical/icosahedral VLPs; black star: crystal structure; white blunt arrow: whorled viroplasm; white exclamation mark: MMV. Inset areas are indicated by white rectangles. From A-R, scale bars are 1 µm, 1 µm, 1 µm, 1 µm, 1 µm, 500 nm, 1 µm, 200 nm, 2 µm, 1 µm, 1 µm, 200 nm, 2 µm, 500 nm, 2 µm, 400 nm, 2 µm, and 400 nm, respectively.

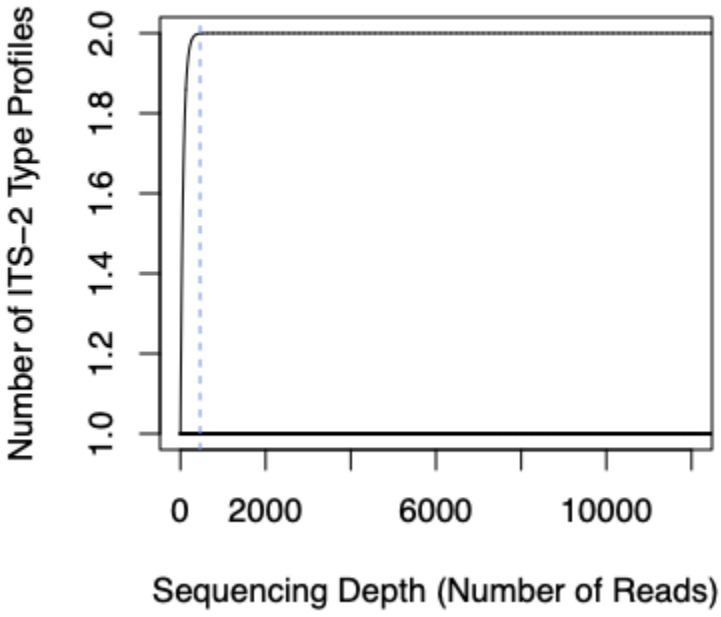

Supplemental Figure 18: Rarefaction curve of the number of Symbiodiniaceae internal transcribed spacer-2 (ITS-2) type profiles by sequencing depth. The blue dashed line is at 461, the minimum number of reads per sample.

Supplemental Figure 19: 16S rRNA gene amplicon sequence variants (ASVs) with >1% abundance in at least one sample. Colors correspond with Figure 5. ASV taxonomy is shown as the Family followed by the genus and species (if known), or the last known rank if Family is undescribed.

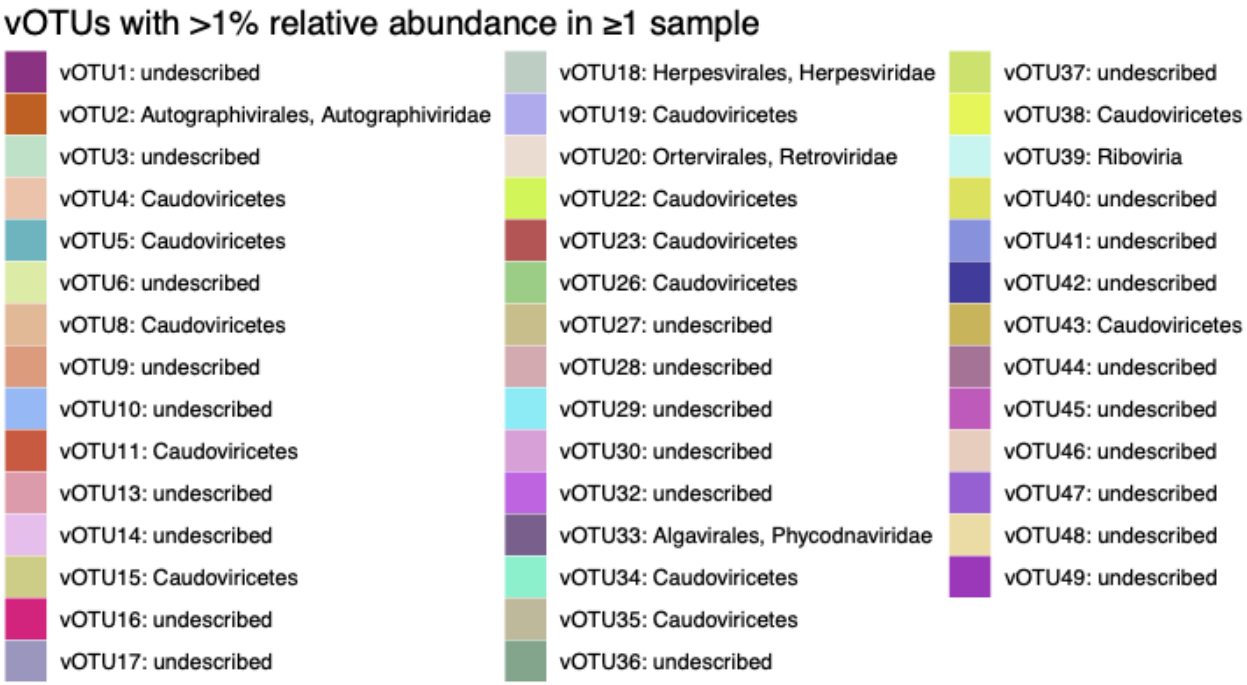

Supplemental Figure 20: Viral operational taxonomic units (vOTUs) with >1% relative abundance in at least one sample. Colors correspond with Figure 5. vOTU taxonomy is shown as the Order followed by the Family, or the last known rank if Family is undescribed.